

2XMM J100451.6+411627*: A cool core cluster at $z = 0.82$

M. Hoeft^{1,2}, G. Lamer², J. Kohnert², and A. Schwobe²

¹ Thüringer Landessternwarte, Sternwarte 5, 07778 Tautenburg, Germany

² Astrophysikalisches Institut Potsdam, An der Sternwarte 16, 14482 Potsdam, Germany

Received; accepted

ABSTRACT

Aims. Gas cooling in the centre of massive galaxy clusters is believed to feed the most powerful active galactic nuclei in the Universe. How often clusters at high redshift show such cool cores has still to be explored by current and upcoming X-ray telescopes.

Methods. We correlated extended X-ray emissions from the second XMM-Newton source catalogue with SDSS data to particularly identify distant clusters. 2XMM J100451.6+411627 is a candidate luminous enough to obtain its redshift and temperature from the X-ray spectrum. We also determine the surface luminosity profile and estimate the temperature in a few spherical bins. The analysis is complemented by a Subaru $g'r'i'$ -image.

Results. 2XMM J100451.6+411627 has a redshift a redshift of $z = 0.82 \pm 0.02$ and a temperature of $k_B T = 4.2 \pm 0.4$ keV. A double- β profile fit yields a highly concentrated surface brightness, $c_{SB} = 0.32$, i.e., the clusters hosts very likely a strong cool core. This is supported by the relaxed morphology of the cluster and an central temperature decrease.

Key words. Galaxies:clusters:individual:2XMM J100451.6+411627 – X-rays:galaxies:clusters

1. Introduction

The space between galaxies in clusters of galaxies is filled with the hot thin intra-cluster medium (ICM). It is heated by merger shocks and adiabatic compression and cools by optically thin thermal plasma emission. Cooling times in the centre of clusters may be shorter than the Hubble time, and as a result some clusters form a cool core. Temperature profiles of local galaxy clusters allow us to distinguish clearly between cool core and non-cool core clusters (Leccardi & Molendi, 2008; Santos et al., 2008; Pratt et al., 2007).

The abundance of cool cores at high redshift may shed light on their formation and on the interaction between the central active galactic nuclei (AGN) and the ICM. The number of cool core clusters at high redshift is still debated. Vikhlinin et al. (2007) argued that galaxy clusters with redshift $z > 0.5$ show a less steep profile at a radius of $0.05 r_{500}$ and concluded by comparison with the profiles of low redshift clusters cluster that cool cores are rare at high redshift. However, Poole et al. (2008) found by numerical simulations that cool cores generally survive cluster mergers. Hence, they may also exists in an epoch of frequent mergers. Recently, Santos et al. (2008) found by evaluating the concentration of the surface brightness for sample of 15 distant galaxy clusters observed with CHANDRA that about 60% of the high- z clusters show at least a mild cool core.

In this paper we report the discovery of a galaxy cluster at $z = 0.82$ in the second XMM-Newton source catalogue (2XMM) that shows a multitude of signs for a strong cool core. In Sec.2 we describe the X-ray properties of 2XMM J100451.6+411627, including the concentration of the surface brightness. In Sec. 3 we describe the observation of the cluster region by the Subaru telescope.

The concordance cosmological parameters $\Omega_M = 0.27$, $\Omega_\Lambda = 0.73$, and $H_0 = 71 \text{ km s}^{-1} \text{ Mpc}^{-1}$ are used throughout this paper. The corresponding linear scale at $z = 0.82$ is $7.6 \text{ kpc}''$. All errors indicate the 1σ uncertainty level, except stated otherwise.

2. X-ray data

The galaxy cluster 2XMM J100451.6+411627 (abbreviated as XMM1004 in the following) was serendipitously detected in XMMEPIC observations of the lensed quasar SDSS J1004+4112 (Observation ID 0207130201, Lamer et al., 2006) and entered the 2XMM catalogue (Watson et al., 2008) as an extended X-ray source. By visual screening we found that XMM1004 is clearly visible in the images of all three EPIC cameras as an extended source, see Fig. 1. The MOS images indicate that the X-ray luminosity of XMM 1004 is very concentrated in the centre.

The position of XMM1004 is covered by the Sloan Digital Sky Survey(SDSS) and in the i -band image one galaxy is marginally detected close to the centroid of the X-ray emission (SDSS 100451.80+411626.6). Therefore the X-ray emission is most likely caused by a distant galaxy cluster.

Send offprint requests to: hoeft@tls-tautenburg.de

* Based on observations obtained with XMM-Newton, an ESA science mission with instruments and contributions directly funded by ESA Member States and NASA

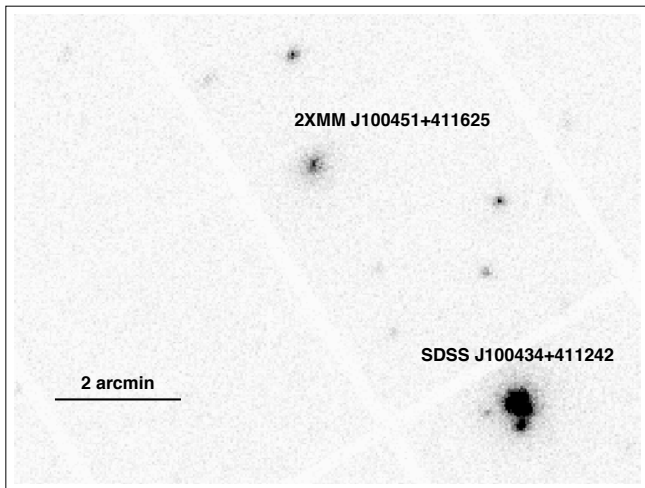


Fig. 1. EPICPN and MOS image of the observation 0207130201 in the 0.2 – 4.5 keV energy band.

With 2500 source counts in the EPICPN camera the source is bright enough to attempt a redshift determination based on the X-ray spectrum. We extract the overall cluster spectrum from a circle with a radius of $50''$ centred on the brightest pixel in the image of the EPICPN camera. On the EPICMOS cameras the chip gap is $23''$ away from the cluster centre. However, we do not expect that the gap significantly affects the spectra and therefore include all three cameras into the spectral analysis.

We use XSPEC version 12.0 to fit a MEKAL plasma model and to subtract the background spectrum. Fits are carried out using the Cash-statistics, which is preferable for low number counts per spectral bin. The galactic neutral hydrogen column density in the direction of XMM 1004 is $N_{\text{H}} = 1.2 \times 10^{20} \text{ cm}^{-2}$, as obtained from radio data¹. The FeK-line is clearly visible at $k_{\text{B}}T = 3.5 \text{ keV}$, see Fig. 2. Hence, the redshift of XMM 1004 is unambiguously determined by the X-ray data. The best-fit redshift, temperature and metallicity are $z = 0.82 \pm 0.02$, $k_{\text{B}}T = 4.2 \pm 0.4 \text{ keV}$, and $Z/Z_{\odot} = 0.5 \pm 0.3$, see Fig. 3.

Our visual inspection indicated that the X-ray luminosity is concentrated to the cluster centre. To quantify the concentration of the surface brightness distribution of XMM 1004 we determined the surface brightness profile. Aiming to deconvolve the intrinsic cluster profile and instrumental point spread function (PSF), we performed a model fitting to the X-ray images. We have used a modified version of the XMM-SAS task `emldetect` to fit two-dimensional models of the X-ray brightness distribution to the combined EPICMOS1 and MOS2 (0.2-4.5 keV) image of XMM 1004. `Emldetect` allows fitting β -models of the form

$$I(x, y) \propto \left(1 + \frac{(x - x_0)^2 + (y - y_0)^2}{r_c^2} \right)^{-3\beta+1/2}$$

where x and y give the coordinates in the image plane and β is fixed at the canonical value $2/3$ for the surface

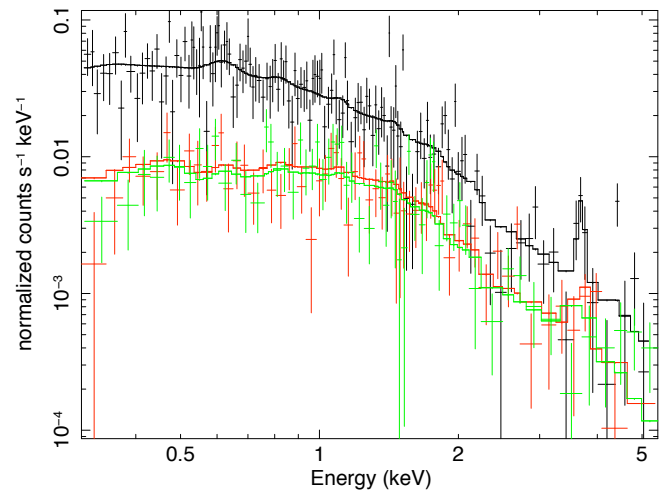


Fig. 2. EPIC MOS (lower spectrum red and green) and the PN (upper spectrum) data with best fitting MEKAL model.

brightness distribution of galaxy clusters. This model is convolved with the instrumental PSF and multiplied with the exposure map of the cameras in each fitting loop. Fitting the luminosity by a single- β model resulted in a systematic discrepancy between the surface luminosity and the fit, see Fig. 4. We therefore used a double- β fit. A modification of `emldetect` was necessary to allow fitting more than one extended source at the same source position, more precisely to fit a double- β profile with two core radii. The model fitting was performed within a radius of $40''$ around the centroid of the cluster X-ray emission.

When the model is constrained to a single radius, the best fitting model has a core radius of $r_c = 8.2''$. A better fit is achieved with a double- β profile and core radii of $r_1 = 2.8''$ and $r_2 = 20''$, where the source with the smaller core radius contributes 44% to the X-ray flux. These radii are consistent with those of nearby cool core clusters, see (Santos et al., 2008). Unfortunately, the angular resolution of XMM-Newton does not allow to exclude a point source

ObsID	0207130201
PN parameters in 2XMM	
ONTIME [s]	41566
OFFAX [arc min]	5.6
CR .2-12 keV [s^{-1}]	0.086 ± 0.002
PN flux in 2XMM	
.2-12 keV [$10^{-13} \text{ erg/cm}^2 \text{ s}$]	1.96 ± 0.13
.5-2 keV [$10^{-13} \text{ erg/cm}^2 \text{ s}$]	0.81 ± 0.02
COUNTS	2448 ± 62
double- β model	
r_{c1} [arc sec]	20.0 ± 1.0
$\int dx dy I_1$	0.0138
r_{c2} [arc sec]	2.8 ± 0.4
$\int dx dy I_2$	0.0107

Table 1. XMM 1004: 2XMM catalogue source parameters and results from the double- β profile fitting using the modified XMM-SAS task `emldetect`.

¹ heasarc.gsfc.nasa.gov/cgi-bin/Tools/w3nh/w3nh.pl

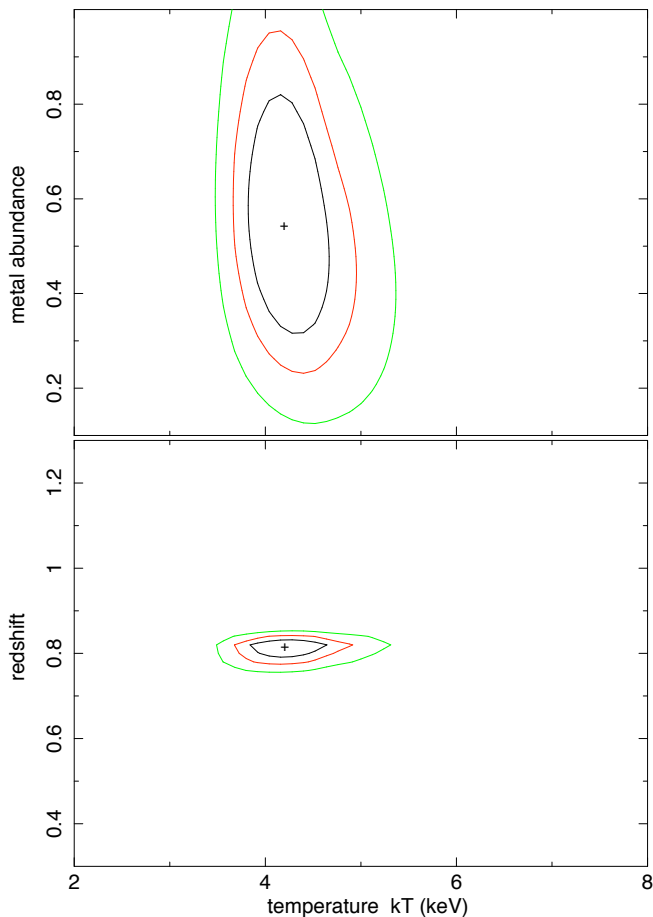


Fig. 3. *Left:* Confidence contours for a fit to the X-ray data using two free parameters, namely redshift and temperature. Starting from the innermost contour, the levels indicate 68%, 90%, and 99% confidence. *Right:* Same confidence contours for metal abundance and temperature.

as origin for the central luminosity excess. Hence, it might alternatively be caused by a luminous AGN. However, the Subaru images show no signs for an AGN in the brightest central cluster galaxy, see Sec. 3.

The background subtracted bolometric X-ray flux as obtained from the MEKAL fit to all three cameras amounts to $F_{\text{bol}} = 1.4 \times 10^{-13} \text{ erg s}^{-1} \text{ cm}^{-2}$ within the aperture of $50''$. Applying the concordance cosmological model allows us to calculate the intrinsic luminosity of the cluster. The used aperture corresponds to a radius of 380 kpc. In contrast, the commonly adopted cluster boundary, r_{500} , amounts to $680 \pm 30 \text{ kpc}$, as obtained from the temperature-radius relation given by O’Hara et al. (2007). The error was estimated by the uncertainty in the temperature determination of XMM1004. From the double- β model fit, see Tab. 1, we derive $L(< r_{500})/L(50'') = 1.13$. As a result, we find for the intrinsic bolometric luminosity of XMM1004 $L_{\text{bol}}(< r_{500}) = 5.3 \times 10^{44} \text{ erg s}^{-1}$.

According to the L - T relation of local galaxy clusters, as derived by Markevitch (1998), the temperature of XMM1004 corresponds to a luminosity of $2.4 \times 10^{44} \text{ erg s}^{-1}$. Thus, XMM1004 is more than twice as luminous as ex-

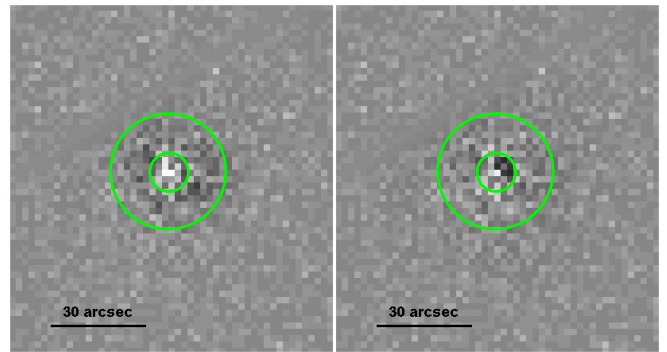


Fig. 4. Residual images after fitting the combined EPIC MOS data with a single- β model (*left*) and a double- β model (*right*) to the combined EPIC MOS data. For the single- β we find an excess emission in the inner circle and a moderately deficient emission in the ring around the inner circle. For the double- β there is no systematic trend (only the absolute noise increases towards the centre).

pected from the low-redshift sample. The redshift evolution of the L - T relation is still under debate. Kotov & Vikhlinin (2005) found that the luminosity scales with $(1+z)^{1.8}$, while O’Hara et al. (2007) report only a moderate evolution. Pacaud et al. (2007) argued that the strong evolution found in earlier works is partially spurious due to selection effects. Taking these into account they found that the luminosity evolves in agreement with predictions based on self-similar cluster evolution. It predicts for $z = 0.82$ a luminosity enhancement factor of 1.4, assuming the concordance cosmology model. Hence, scaling the luminosity of XMM1004 according to self-similar cluster evolution keeps it over-luminous by a factor of 1.5 compared to a local cluster sample. For local clusters it is known that the luminosity may be enhanced by a cool core, what may be also the case for XMM1004.

Santos et al. (2008) introduced the surface brightness concentration, c_{SB} , as a measure for the presence of a cool core. The concentration gives the ratio of the luminosities within 40 and 400 kpc. For XMM1004 40 kpc corresponds to $5.3''$. We cannot determine the concentration from the cluster image directly, since the EPIC MOS cameras smooth the image substantially. More precisely, the FWHM of the PSF is $9''$ at the off-axis angle of XMM1004. Therefore, we use the results of the double- β model fit which provides a the deconvolved surface brightness profile. With this the surface brightness concentration of XMM1004 amounts to $c_{\text{SB}} = 0.32$. This is a higher concentration than Santos et al. (2008) derived for any cluster in their sample including the local clusters. This clearly marks XMM1004 as a candidate for a strong cool core cluster at high redshift.

Radial temperature profiles are routinely derived for local clusters (Pratt et al., 2007). However, a large photon number is needed in order to extract the temperature from the spectrum computed for different regions. This may get even more difficult in merging clusters, which may show a very complex temperature distribution. Cool core clusters in contrast are generally relaxed systems,

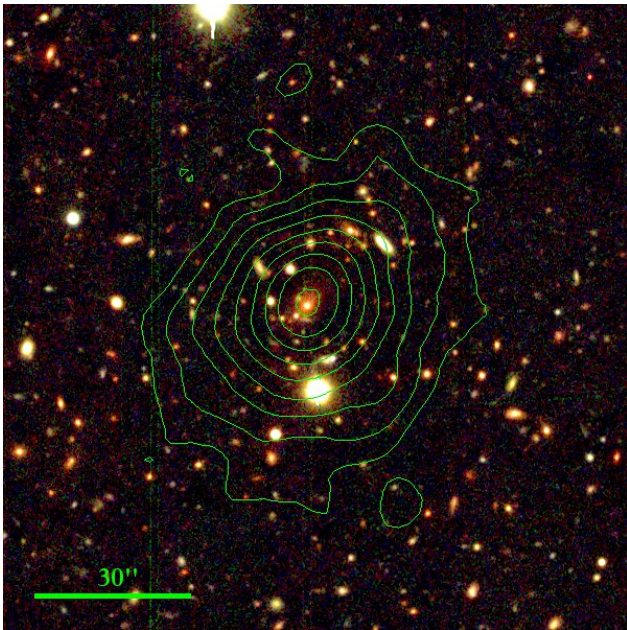


Fig. 5. Subaru $g'r'i'$ -colour-composite image with EPIC PN X-ray contours of XMM1004 overlaid.

hence a spherically symmetric morphology is expected and is indeed found for XMM1004, see Fig. 5. Therefore we subdivide the area of XMM1004 into four radial bins, enclosing in each bin a similar number of source photons. In each bin we fit the spectrum in a photon energy range from 0.3 to 7 keV, strictly excluding all time intervals with a flare of energetic particles, noticeable in the energy band above 10 keV. We assume for all bins a common redshift and metallicity as derived for the entire cluster. Fig. 6 shows the resulting temperatures in the four bins. In the inner region the temperature decreases by about 30%, as it is known for low redshift cool core clusters. XMM1004 is therefore the most distant cluster with a cool core verifiable by the temperature profile to date.

The mass of a cluster can be estimated by assuming hydrostatical equilibrium and spherical symmetry and the average cluster temperature

$$M_{500} \sim \frac{3\beta}{G} \frac{k_B T r_{500}}{\mu m_p}.$$

With $\beta = 0.66$ and $\mu = 0.6$ we obtain for the cluster mass $M_{500} = (2.0 \pm 0.3) \times 10^{14} M_\odot$. The mass-temperature relation of Vikhlinin et al. (2006) predicts $M_{500} = (1.4 \pm 0.2) \times 10^{14} M_\odot$, which is within 3σ of our derived value.

3. Subaru images

The field has also been observed with the Subaru Suprime-Cam imager in the g' , r' , i' , and z' -band, targeted on the lens system SDSS J100434+411242. The respective exposure times were 810s, 1210s, 1340s, and 180s. We retrieved the data from the SMOKA archive and used the SDFRED pipeline (Yagi et al., 2002) for the reduction of the g' , r' and i' images. We used point sources from the

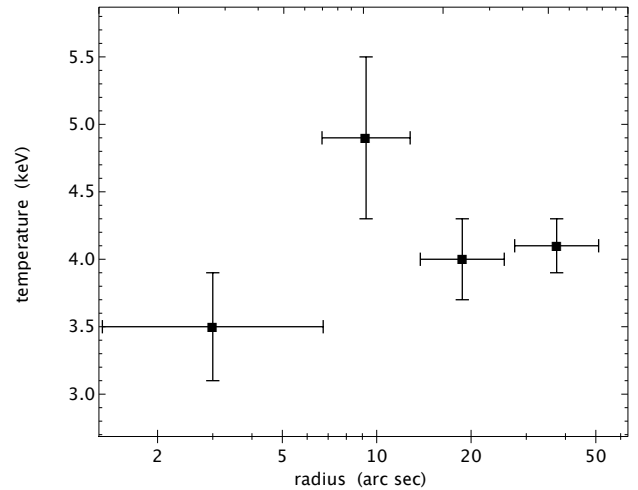


Fig. 6. Temperature in four radial bin, using the PN and the MOS cameras.

SDSS for the astrometric and photometric calibration of the Suprime-Cam data. The image quality of the reduced images is FWHM = $0.66''$ in the g' -band image, $0.78''$ in the r' -band and $0.73''$ in the i' -band.

The Subaru images reveal a clear overdensity of red galaxies within the X-ray contours. The brightest cluster galaxy (BCG) is located close to the centroid of the X-ray emission, see Fig. 5, indicating that XMM1004 has a very relaxed morphology. The $r' - i'$ vs. i' colour-magnitude diagram, see Fig. 7 of the galaxies close to the X-ray position shows a distinct red sequence with $r' - i' \sim 1.4$. The BCG is aligned with the red sequence, rendering a luminous AGN as source for the central X-ray luminosity excess unlikely.

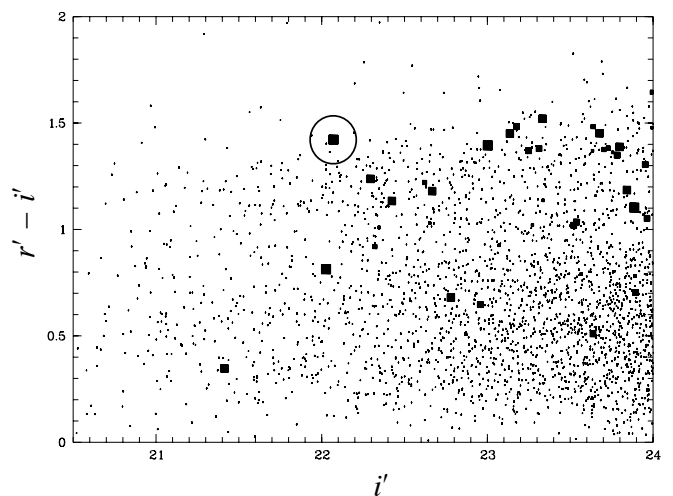


Fig. 7. Colour-magnitude-diagramme of XMM1004. Larger symbols indicate lesser distance of the objects to the X-ray centre of the cluster. The BCG is encircled.

4. Summary

Based on X-ray data we show that XMM1004 is a luminous cluster at redshift $z = 0.82 \pm 0.02$ and with the help of a MEKAL fit we determine its temperature, $k_{\text{B}}T = 4.2 \pm 0.4$ keV. The surface luminosity of the cluster is exceptionally concentrated, $c_{\text{SB}} = 0.32$, compared to other distant galaxy clusters (Santos et al., 2008). This suggests that XMM1004 hosts a strong cool core. A decreasing temperature in the centre and the extremely relaxed morphology of the cluster may serve as further pieces of evidence for a strong cool core cluster in the distant Universe.

Acknowledgements. JK is supported by the DFG priority programme STP1177 (grant no. SCHW563/23-1). MH acknowledge support by the Deutsches Zentrum für Luft- und Raumfahrt (DLR) under contract no. FKZ 50 OX 0201. This work is based on observations obtained with XMM-Newton.

References

- Kotov, O., & Vikhlinin, A. 2005, ApJ, 633, 781
- Lamer, G., Schwobe, A., Wisotzki, L., & Christensen, L. 2006, A&A, 454, 493
- Leccardi, A., & Molendi, S. 2008, A&A, 486, 359
- Markevitch, M. 1998, ApJ, 504, 27
- O’Hara, T. B., Mohr, J. J., & Sanderson, A. J. R. 2007, ArXiv e-prints, 710
- Pacaud, F., Pierre, M., Adami, C., Altieri, B., Andreon, S., Chiappetti, L., Detal, A., Duc, P.-A., Galaz, G., Gueguen, A., Le Fèvre, J.-P., Hertling, G., Libbrecht, C., Melin, J.-B., Ponman, T. J., Quintana, H., Refregier, A., Sprimont, P.-G., Surdej, J., Valtchanov, I., Willis, J. P., Alloin, D., Birkinshaw, M., Bremer, M. N., Garcet, O., Jean, C., Jones, L. R., Le Fèvre, O., Maccagni, D., Mazure, A., Proust, D., Röttgering, H. J. A., & Trinchieri, G. 2007, MNRAS, 382, 1289
- Poole, G. B., Babul, A., McCarthy, I. G., Sanderson, A. J. R., & Fardal, M. A. 2008, ArXiv e-prints, 804
- Pratt, G. W., Böhringer, H., Croston, J. H., Arnaud, M., Borgani, S., Finoguenov, A., & Temple, R. F. 2007, A&A, 461, 71
- Santos, J. S., Rosati, P., Tozzi, P., Böhringer, H., Ettori, S., & Bignamini, A. 2008, A&A, 483, 35
- Vikhlinin, A., Burenin, R., Forman, W. R., Jones, C., Hornstrup, A., Murray, S. S., & Quintana, H. 2007, in Heating versus Cooling in Galaxies and Clusters of Galaxies, ed. H. Böhringer, G. W. Pratt, A. Finoguenov, & P. Schuecker, 48–+
- Vikhlinin, A., Kravtsov, A., Forman, W., Jones, C., Markevitch, M., Murray, S. S., & Van Speybroeck, L. 2006, ApJ, 640, 691
- Watson, M. G., Schröder, A. C., Fyfe, D., Page, C. G., Lamer, G., Mateos, S., Pye, J., Sakano, M., Rosen, S., Ballet, J., Barcons, X., Barret, D., Boller, T., Brunner, H., Brusa, M., Caccianiga, A., Carrera, F. J., Ceballos, M., Della Ceca, R., Denby, M., Denkinson, G., Dupuy, S., Farrell, S., Frascchetti, F., Freyberg, M. J., Guillout, P., Hambaryan, V., Maccacaro, T., Mathiesen, B., McMahon, R., Michel, L., Motch, C., Osborne, J. P., Page, M., Pakull, M. W., Pietsch, W., Saxton, R., Schwobe, A., Severgnini, P., Simpson, M., Sironi, G., Stewart, G., Stewart, I. M., Stobbart, A., Tedds, J., Warwick, R., Webb, N., West, R., Worrall, D., & Yuan, W. 2008, ArXiv e-prints, 807
- Yagi, M., Kashikawa, N., Sekiguchi, M., Doi, M., Yasuda, N., Shimasaku, K., & Okamura, S. 2002, AJ, 123, 66

List of Objects

‘SDSS J100434+411242’ on page 4